AIR INLETS

By Norman F. Smith

Langley Aeronautical Laboratory

The first radial-engine cowling, developed by the NACA in 1927 (fig. 1), marked the transition from the external to the internal cooling system. This development provided an important improvement in airplane performance by removing engine and heat-exchanger components, which are poor aerodynamic shapes, from the full velocity of the air stream and by providing gains in cooling efficiency and control of engine temperature.

Some years later, airplane speeds had advanced to the point where the critical speed of components became important. The critical speed of the original cowling was recognized as being low, and an investigation was initiated in 1939 to develop a shape having as high a critical speed as possible and proportions to fit then-existing radial engines. The result of this effort was NACA cowling C (fig. 1), which has a critical Mach number of 0.63 (480 mph at sea level) and has been virtually a standard on American radial-engine aircraft since its development (reference 1). A short time later, nose B was developed (reference 2 and fig. 1). This shape is a longer nose inlet designed for use with submerged engine designs or jet propulsion installations, and has a critical Mach number of 0.84 (640 mph at sea level). These two inlets, NACA cowling C and nose B, were derived on the same basis, that is, to have a flat pressure distribution and, therefore, the optimum critical speed for the particular proportions involved.

The fuselage nose position for air inlets has received considerable attention at the Langley Laboratory because of the aerodynamic advantages offered by this position. Such an air intake is located in a natural stagnation region wherein external compression can be accomplished at an efficiency of 100 percent. Also, no boundary-layer problem is encountered, and there exists the fact that the external drag of a body with a properly designed nose inlet is as low as or lower than the drag of a streamlined body. Experimental data (from reference 2) illustrating this last item are shown in figure 2. The tick at the left is the drag coefficient of the basic body, whereas the curve shows the external drag of the body with nose B inlet through a range of internal flow. At flow rates above a certain minimum value, the external drag is clearly seen to be equal to or slightly less than the drag of the basic body. The higher drag at low flow rates is due to the fact that a pressure peak exists at the lip for this condition, and this peak fixes transition at a point well forward and produces higher skin-friction drag.

From the aircraft designer's point of view, it was highly
desirable to expand the information available on nose inlets to permit
design of a nose inlet for any desired subsonic Mach number. Upon
examination, the nose B and NACA cowling C ordinates, reduced to
nondimensional form, were found to be practically the same. Since
the very different critical speeds of these air inlets were apparently
due to the different geometric proportions, it appeared possible that
a whole series of nose inlets might be based upon common ordinates.
By use of the nose B ordinates, therefore, the systematic family of nose
inlets shown in figure 3 was designed and was tested to determine the
effects of proportions on critical speed characteristics (reference 3).
The length ratio (X/D) is shown across the top and the inlet diameter
ratio d/D down the side. The inlet shown in the upper left is
approximately nose B, whereas the one in the lower right is very close
to NACA cowling C.

The results of tests of one of these nose inlets are shown in
figure 4. In the left figure are the pressure distributions over the
external surface of the inlet at three values of inlet velocity ratio,
which is the ratio of inlet velocity to free-stream velocity. It can
be seen that the pressure distribution remains flat, with a low peak
value, down to some low value of V_1/V_0, below which the high local
angle of attack of the lip causes a pressure peak to occur. This peak
continues to increase in height as V_1/V_0 is further decreased. The
estimated critical Mach numbers obtained from these pressure distri-
butions are shown in the right half of figure 4 plotted against inlet-
velocity ratio. It can be seen that the critical Mach number of the
nose inlet remains approximately constant as the inlet-velocity ratio
is decreased until the point is reached where a pressure peak appears
at the lip. Below this value of inlet-velocity ratio, the critical
Mach number decreases rapidly.

The values of critical Mach number below the "knee" of the curve
are of course in need of qualification because they were estimated
from sharp local peak pressures, and it has been shown in various
wind-tunnel tests of airfoils and bodies that such local peaks may
disappear at higher Mach numbers or have little effect upon the Mach
number at which adverse compressibility effects occur. This phenomenon
is discussed in connection with airfoils in the paper by Becker
entitled "Characteristics of Wing Sections at Transonic Speeds." It
is, however, desirable aerodynamically to avoid this condition for
reasons of possible compressibility effects, separation, or, as was
shown in figure 2, higher skin friction.

The region to the right of the knee of the critical Mach number
curve of figure 4, therefore, is of primary interest. Since in most
airplane installations the minimum inlet-velocity ratio is encountered
at the maximum speed of the airplane, the knee of the curve becomes

a logical "design point" for the particular nose inlet. In other words, an airplane for which maximum Mach number and air-flow requirements at the maximum Mach number correspond to the "knee" of the curve will, at speeds other than maximum, be operating below and to the right of the design point in the region where a flat pressure distribution exists.

The values of M_{cr} and V_1/V_0 at the design point was found in the wind-tunnel tests to be a function of the proportions of the nose inlet. Accordingly, the design points of the series of nose inlets shown in figure 3 have been arranged in the form of design charts, from which the proportions of a nose inlet can be selected to fulfill any design requirements of air flow and critical Mach number. The design chart is shown as figure 5. A sample selection is shown by the arrows. Entering the lower section with the desired value of mass flow ratio and proceeding vertically to the value of critical Mach number desired, the entrance diameter ratio d/D can be read. Continuing to the top section of the chart, the length ratio X/D is obtained. Combining these proportions with the 1-series ordinates the required nose inlet shown at left center is obtained. Two other selections, for Mach numbers of approximately 0.63 and 0.9, are shown to scale and illustrate the variation in proportions with Mach number.

The design charts actually cover a number of different types of inlets, the first of which is of course the plain open-nose inlet as applied to a jet machine. Mention has been made previously of the excellent drag characteristics of this type of installation.

Two additional types of installations which can be designed from these charts are shown in figure 6. The upper one is a more or less conventional configuration where the propeller is located on a spinner ahead of the air inlet. An analysis (reference 3) of existing data from various cowling tests provides an indication that the effects of a spinner of reasonable size upon the characteristics of a cowling are small. Cowlings for use with spinners can therefore be selected from the design charts, taking into account only the flow area blocked out by the spinner. An additional problem exists with this type of inlet, however, in that the boundary layer on the spinner will separate if the inlet-velocity ratio is too low. This phenomenon is purely a result of the pressure gradient ahead of the air inlet, produced principally by the inlet-velocity ratio. Analysis (reference 3) of data from tests of many cowlings indicates that a value of inlet-velocity ratio of at least 0.4 is required to eliminate separation from the spinner. This value is, of course, higher than that which might otherwise be used in order to minimize internal losses. More on this problem is presented herein in connection with fuselage scoops.

The lower installation shown in figure 6 is an NACA rotating cowling in which the forward part of the cowling rotates with the

propeller (reference 4). Although more complicated mechanically, this type of installation offers several aerodynamic advantages. The problem of boundary—layer separation at the entrance (due to inlet—velocity ratio) is eliminated since no surface protrudes beyond the inlet. Also, the propeller shanks, which are often difficult to make optimum both aerodynamically and structurally, can be housed in generous fairings in the lower velocity region within the spinner. By this means, the internal efficiency is improved, particularly on installations of high power where a large number of wide blades are needed. The propulsive efficiency is also improved because only the more efficient outboard sections of the propeller are exposed to the air stream. Several tests of these types of installations have indicated that the aerodynamic advantages of the rotating type are larger than the weight and structural penalties incurred, particularly for installations of very high power.

Another type of "stagnation inlet" is, of course, the wing—leading—edge inlet. The problems involved in the design of wing inlets are more numerous than for other types. The effective—angle—of—attack range through which the inlet must operate is higher because of the induced angle of attack which occurs ahead of the wing. If the inlet is located behind a propeller, the effective angle will also be affected by propeller power. The inlet must have a high critical Mach number at one end of the speed range and a high value of maximum lift at the other, while maintaining reasonable drag characteristics through—out the operational range of lift coefficient and inlet—velocity ratio. The wing inlet is of interest primarily for aircraft having wings of high or medium thickness since the very thin wings of high—speed aircraft do not offer the thickness or internal space for inducting the large volume of air required.

Because of the large number of variables and problems involved, design data for wing inlets are not available from which an inlet can be chosen without a development program being required. However, the general physical configuration required for satisfactory characteristics is known from numerous development programs. Figure 7 compares such a configuration (reference 5) with an earlier and less satisfactory development (reference 6). The early inlet shown in the sketch at the lower left is characterized by relatively sharp lips, a large opening height, and no lip stagger. The pressure distribution over the upper lip at zero lift is flat, with a value of peak pressure which, although not shown, appears low. At a lift coefficient of 0.55, however, a high pressure peak exists at the lip, which is undesirable from the standpoint of drag (transition), critical speed, and, at a still higher angle of attack, maximum lift.

The inlet at the right shows a more rounded pressure distribution, although a slightly higher value of peak pressure, and it evinces only a small pressure peak at a lift coefficient of 0.66. This inlet possesses thicker lips, a small inlet height, and a noticeable lip stagger.

The maximum lift characteristics of these two configurations and of a basic airfoil section are shown in the left half of figure 8. As might be expected, the sharp-edge inlet (a) has a very low maximum lift at low flow rates, rising to about the same as the basic airfoil section when the favorable effects of air flow are felt at the higher inlet-velocity ratios. The air inlet (b) has a higher maximum lift than inlet (a) or the basic airfoil section through a wide range of air-flow quantity.

The inlet losses for inlets (a) and (b) are shown in the right half of figure 8. Again, the sharp lips of inlet (a) have produced large losses outside a narrow range of lift coefficient. Inlet (b), however, shows essentially zero inlet losses through a wide range of lift coefficient, adequate for the particular airplane involved.

Thus, a wing-leading-edge inlet which has good aerodynamic characteristics has a small entrance-to-thickness ratio and relatively thick, staggered inlet lips well-rounded into a bell-mouth shape.

Several advantages of the stagnation type of air inlet have already been listed and discussed. In spite of these advantages, it often happens that other factors dictate the use of an air scoop or air inlet located aft on the fuselage. Such factors may include armament in the nose, pilot visibility, ducting length and weight, over-all structural weight, and airplane stability.

The two primary problems involved in scoop design are boundary layer and interference. Figure 9 illustrates the boundary-layer phenomena (reference 7). In the upper left is a sketch of a fuselage and scoop. Below the sketch is plotted the boundary-layer thickness along the fuselage ahead of the scoop for three values of inlet-velocity ratio. At the highest value, 0.9, the boundary layer grows at a normal rate up to the scoop entrance. At an inlet-velocity ratio of 0.5 some thickening at the entrance is found; and at the lowest inlet-velocity ratio, 0.2, the boundary layer has apparently separated and has reached a thickness equal almost to the scoop entrance height. A cross plot of the boundary-layer thickness shown at the right indicates that separation apparently occurs when the inlet-velocity ratio is decreased below approximately 0.6. This phenomenon is the same as that which was previously mentioned as occurring on cowling spinners. The consequences of the separation shown were, of course, a reduction in air-flow quantity and a substantial increase in inlet losses. Providing the scoop shown with a boundary-layer bypass which removed a thickness slightly more than the boundary-layer thickness for $\dfrac{V_1}{V_0} = 0.9$ eliminated the separation entirely and restored the pressure recovery to essentially 100 percent.

In figure 10 (from reference 3) is shown the critical Mach number characteristics of three longitudinal planes of the scoop with boundary-layer removed: the bottom plane, shown by the solid line, the side plane, shown by short dashes, and the fillet plane, shown by long dashes. The scoop was designed by use of the NACA 1—series nose inlet ordinates. For comparison, the critical Mach number curve for the corresponding NACA 1—series nose inlet is shown as the top curve. The curves for the two lower planes have essentially the same shape as the curve for the nose inlet but are displaced downward because the scoop is located in the flow field of the wing. The curve for the fillet plane is displaced still farther and its shape is changed somewhat. These data show that the external contour of a fuselage scoop can be designed with the aid of the NACA 1—series nose inlet charts provided that proper allowance is made for the interference of wing or fuselage.

While problems do exist in the design of efficient air exits, their magnitude and number are by no means comparable to those involved in the design of air inlets. The optimum location for emitting air is, of course, at the tail of the fuselage or body, since here mutual interference of fuselage and the air jet are minimized. In cases where the air exit must be located elsewhere, a few simple rules should be followed: First, the air exit should be located in a region of low induced velocity to minimize interference effects; second, the air should be directed outward parallel to the passing air stream; and third, the body aft of the exit should be undercut to allow for the thickening effect of the air jet.

Figure 11 illustrates this third item and shows pressure distributions over an air exit with and without undercutting (reference 8). It should be noted that a pressure peak (solid line) is induced at the exit by the effective bump produced by the mass of air flowing from the exit. Undercutting the exit (dashed line) reduced this peak to only a small increment above the value of pressure coefficient measured with the exit faired over. Doubtless, this dashed profile could be improved by still more undercutting and the superstream velocities eliminated altogether, at least for certain operating conditions.

Although this paper deals primarily with the subject of air inlets, it is appropriate to include several references on duct and internal-system design (references 9 to 11). These references do not in themselves constitute complete coverage of the subject, but, like many of those listed at the end of this paper, provide a digest of much of the available information. Each paper contains a list of references which may be used in an extended study of the subject.

In considering briefly the problem of supersonic air inlets, it is interesting to consider the case of a subsonic nose inlet operating at transonic and supersonic speeds. (See fig. 12.) At supersonic

speeds, a conventional nose inlet with rounded lips is found to have a bow wave ahead. Through this bow wave there is a loss in total pressure of the air, both that entering the inlet and that going around the body. The total pressure loss through a normal shock, which approximates the loss through the center part of a bow wave, is shown in the upper right corner of figure 12. It can be seen that the loss is small at low supersonic Mach numbers — of the order of 2 percent at $M = 1.3$. This means that the losses encountered at low supersonic Mach numbers with this type of inlet will be small. This inlet is suitable for use, then, in the transonic range, with the added advantage of good characteristics through the subsonic range.

At higher supersonic Mach numbers, however, the losses increase significantly, and other types of inlets must be considered. If the blunt lips of the subsonic inlet are replaced with suitable sharp-edged lips and if the inlet—velocity ratio is increased to 1.0, the bow wave may be eliminated and replaced by an external oblique shock and by a normal shock in the diffuser, as shown in the lower half of figure 12.

If a normal diverging subsonic diffuser is used, the shock will occur at a Mach number equal to or higher than the flight Mach number. This means that, although the external conditions may be improved by using this type of inlet, the internal losses will be higher than for the subsonic configuration of figure 12.

The configuration shown in figure 13 incorporates a converging—diverging diffuser (reference 12) in an attempt to compress the flow supersonically and cause the shock in the diffuser to occur at a lower Mach number.

The upper curve at the right gives the contraction ratio between entrance and throat for isentropic compression to $M = 1$ at the throat. This throat area is, however, too small for the establishment of supersonic flow in the converging section, since in order to "swallow" the shock, the throat must first pass the mass flow required for an inlet—velocity ratio of unity at the reduced density and total pressure due to the bow wave. The lower curve gives the maximum contraction ratio which can be used if a diffuser is to start or "swallow" the shock. The permissible contraction ratio is seen to be about half that required at $M = 1.6$ and less at higher Mach numbers. Thus, the requirements for starting a converging—diverging diffuser reduce the effectiveness of this configuration seriously in that large losses are still encountered through the normal shock in the diffuser at higher supersonic Mach numbers.

The type of air inlet shown schematically at the lower left was suggested by Oswatitsch in Germany (reference 13) and makes use of the more efficient compression through several oblique shocks on a conical body ahead of the inlet. After compression to a low supersonic Mach

number ahead of the entrance, the flow enters a converging—diverging diffuser in which a normal shock occurs as in the previous case, but at a very low supersonic Mach number with, of course, improved pressure recovery.

The following statements are made in summary:

Design charts are available from which optimum-critical-speed nose inlets can be selected for any required subsonic Mach number. These charts may also be used in the design of rotating cowlings, cowlings for use with spinners, and to aid in the design of fuselage scoop contours. In configurations where boundary layer exists ahead of an air inlet, either the inlet—velocity ratio must be kept high enough to prevent separation or a suitable scoop or bypass must be provided to remove the boundary layer.

Wing-inlet shapes have been developed which have maximum lift higher than plain airfoil sections and which have critical Mach number and internal pressure—recovery characteristics adequate for the airplanes involved.

The subsonic nose inlet can be used effectively at low supersonic Mach numbers because losses through the normal shock (or bow wave) are small at low supersonic Mach numbers. At higher supersonic Mach numbers a different configuration is needed which has sharp leading edges and which utilizes the most efficient arrangement of shocks possible for compressing the inlet flow. One such configuration utilizes a series of oblique shocks on a central conical body for compression to low supersonic Mach numbers ahead of the inlet.

REFERENCES

1. Robinson, Russell G., and Becker, John V.: High—Speed Tests of
   Conventional Radial—Engine Cowlings. NACA Rep. No. 745, 1942.

2. Becker, John V.: Wind—Tunnel Tests of Air Inlet and Outlet
   Openings on a Streamline Body. NACA ACR, Nov. 1940.

3. Baals, Donald D., Smith, Norman F., and Wright, John B.: The
   Development and Application of High—Critical—Speed Nose Inlets.
   NACA ACR No. L5F30a, 1945.

4. McHugh, James G.: Progress Report on Cowlings for Air—Cooled
   Engines Investigated in the NACA 19—Foot Pressure Wind Tunnel.
   NACA ARR, July 1941.

5. Racisz, Stanley F.: Development of Wing Inlets. NACA ACR No. L6B18,
   1946.

6. Smith, Norman F.: High—Speed Investigation of Low—Drag Wing Inlets.
   NACA ACR No. L4I18, 1944.

7. Smith, Norman F., and Baals, Donald D.: Wind—Tunnel Investigation
   of a High—Critical—Speed Fuselage Scoop Including the Effects of
   Boundary Layer. NACA ACR No. L5B01a, 1945.

8. Becker, John V., and Baals, Donald D.: Wind—Tunnel Tests of a
   Submerged—Engine Fuselage Design. NACA ACR, Oct. 1940.

9. Rubert, Kennedy F., and Knopf, George S.: A Method for the Design
   of Cooling Systems for Aircraft Power—Plant Installations.
   NACA ARR, March 1942.

10. Becker, John V., and Baals, Donald D.: Analysis of Heat and
    Compressibility Effects in Internal Flow Systems and High—Speed
    Tests of a Ram—Jet System. NACA ACR, Sept. 1942.

11. Henry, John R.: Design of Power—Plant Installations. Pressure—
    Loss Characteristics of Duct Components. NACA ARR No. L4F26, 1944.

12. Kantrowitz, Arthur, and Donaldson, Coleman duP: Preliminary
    Investigation of Supersonic Diffusers. NACA ACR No. L5D20, 1945.

13. Oswatitsch, Kl.: Pressure Recovery for Missiles with Reaction
    Propulsion at High Supersonic Speeds (The Efficiency of Shock
    Diffusers). NACA TM No. 1140, 1947.

ORIGINAL NACA COWLING

NACA COWLING C

NACA COWLING B
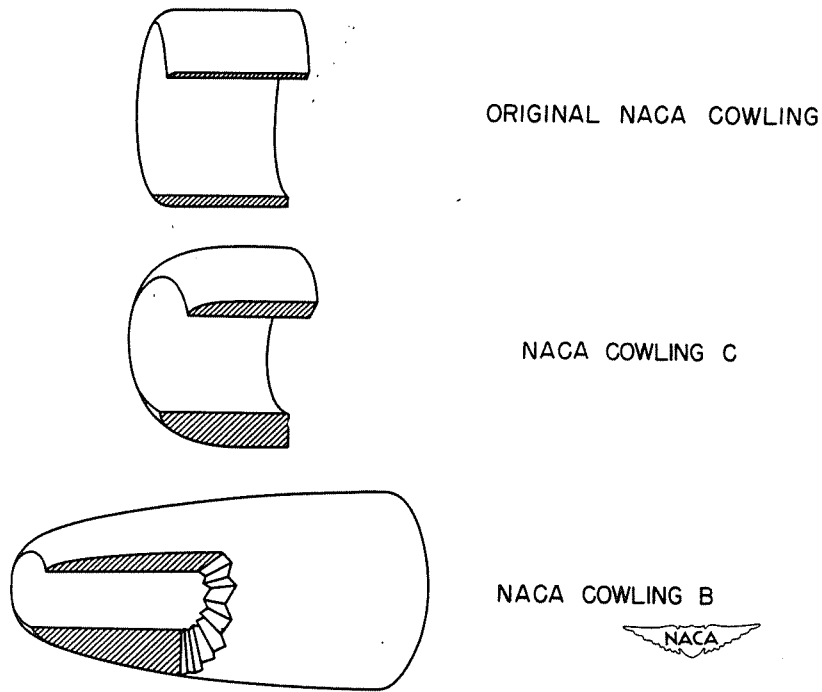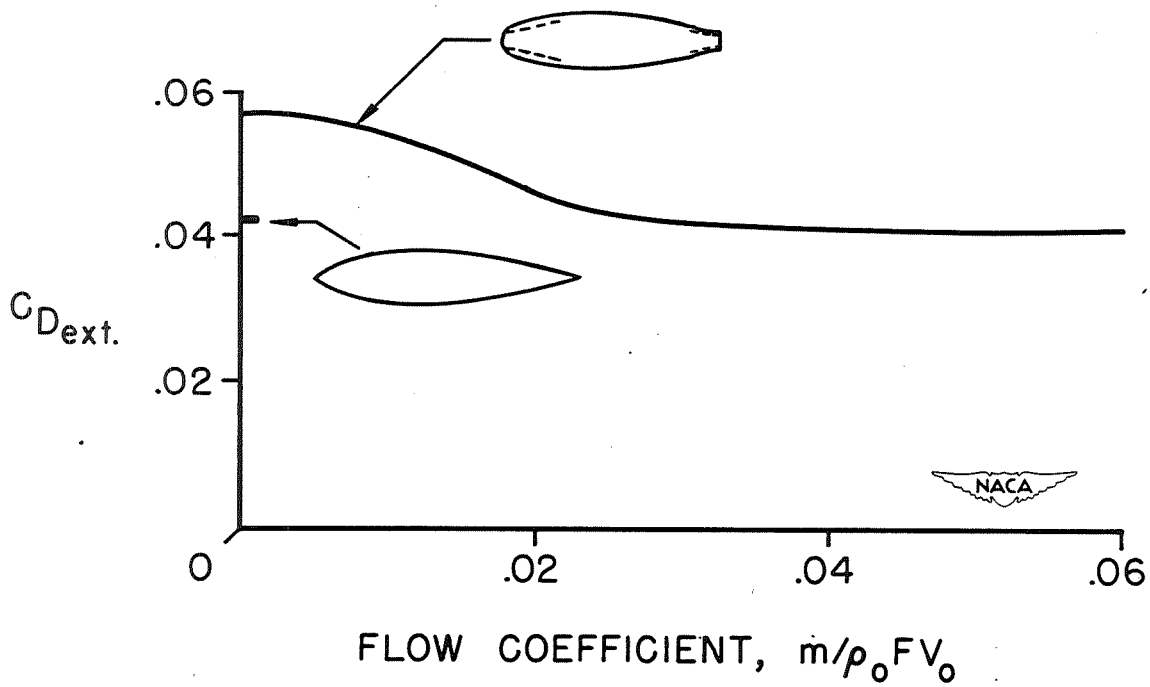
Figure 1.

Figure 2.- External drag of body with and without nose inlet.
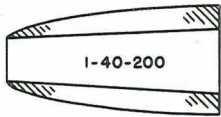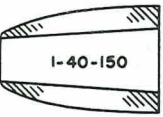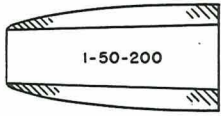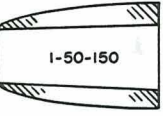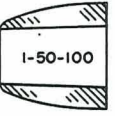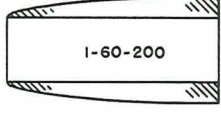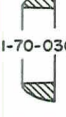
d/D	X/D					
	2.00	1.50	1.00	0.75	0.50	0.30
0.40	1-40-200	1-40-150				
0.50	1-50-200	1-50-150	1-50-100		1-50-050	
0.60	1-60-200	1-60-150	1-60-100	1-60-075	1-60-050	
0.70		1-70-150	1-70-100		1-70-050	1-70-030

NACA

Figure 3.- NACA 1-series nose inlets tested.

NOSE INLET OUTLINE

V_1/V_0

0.20
.44
.98

$\alpha = 0°$
$M = 0.4$

α
0°
2°

NACA

INLET VELOCITY
RATIO V_1/V_0
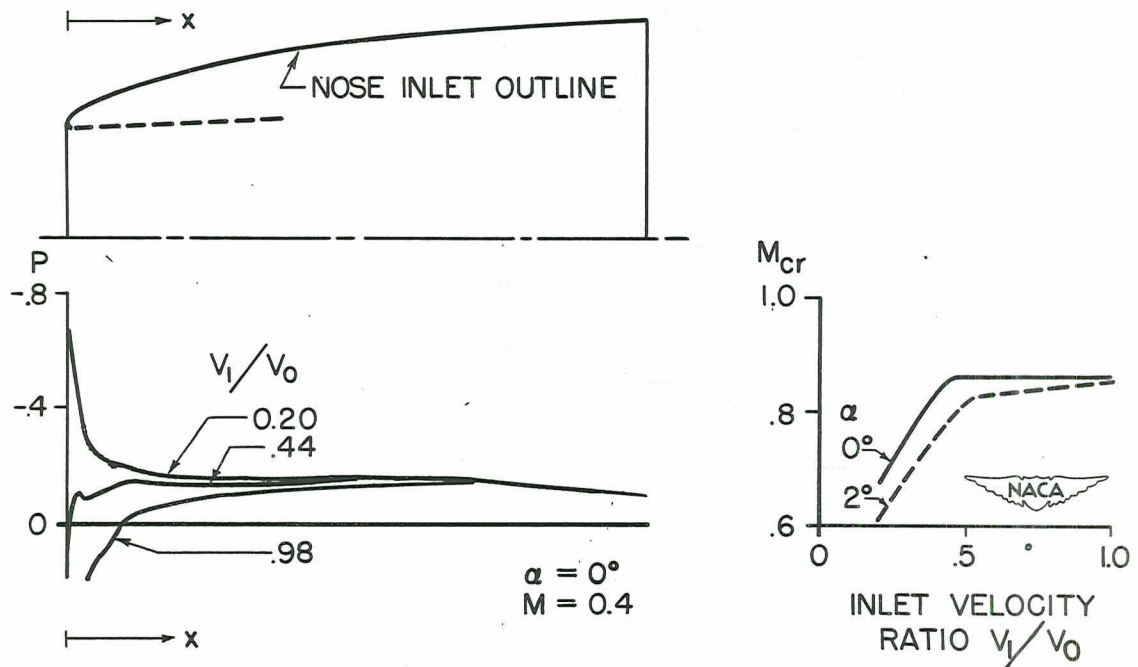
Figure 4.- Characteristics of typical NACA 1-series nose inlet. (1-50-150).

318
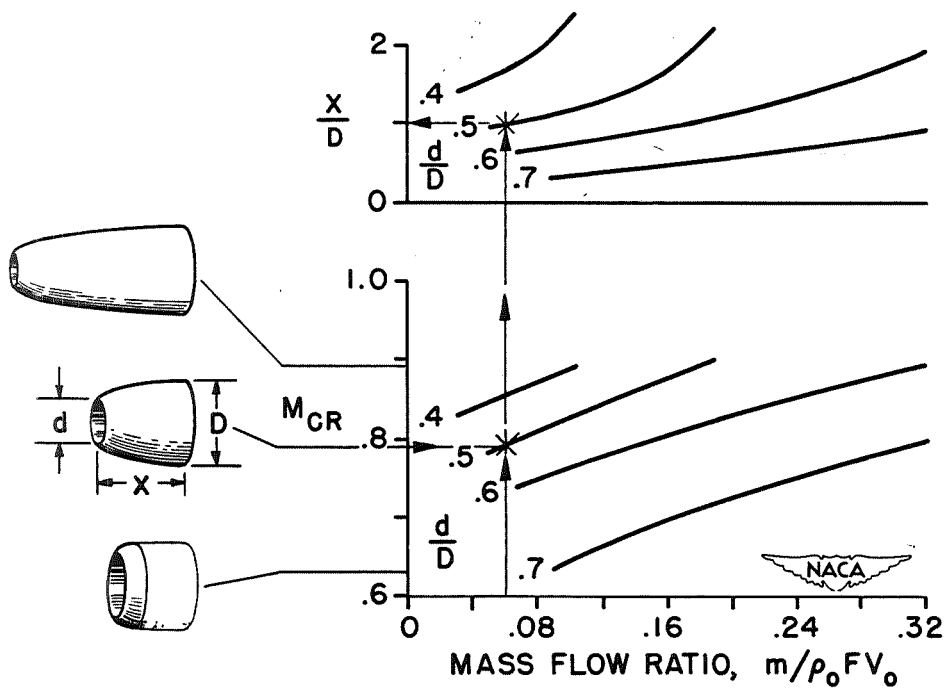
Figure 5.- NACA 1-series design chart.

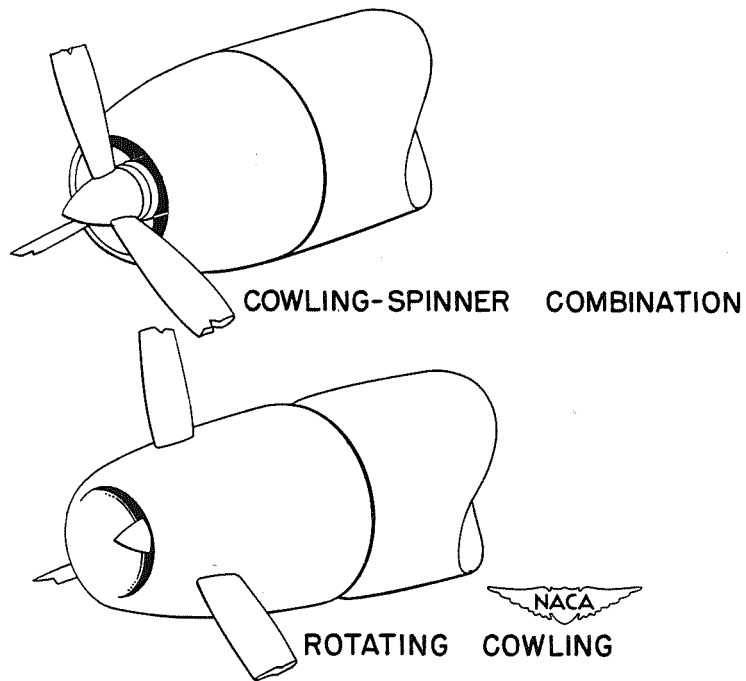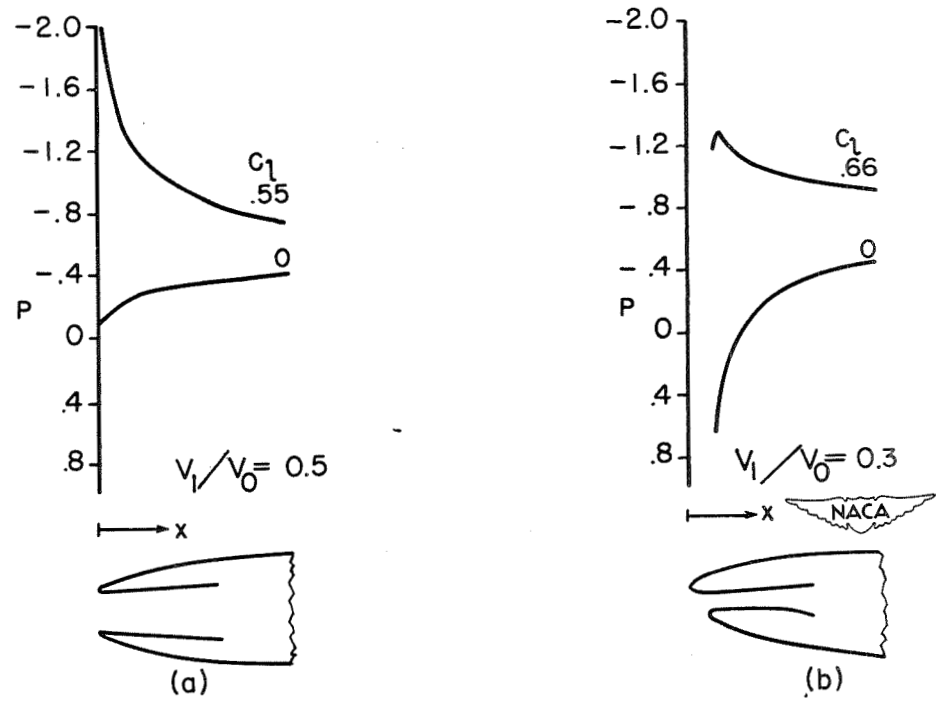
COWLING-SPINNER COMBINATION

ROTATING COWLING

Figure 6.

319

Figure 7.- Pressure distributions over upper lip of two wing inlets.
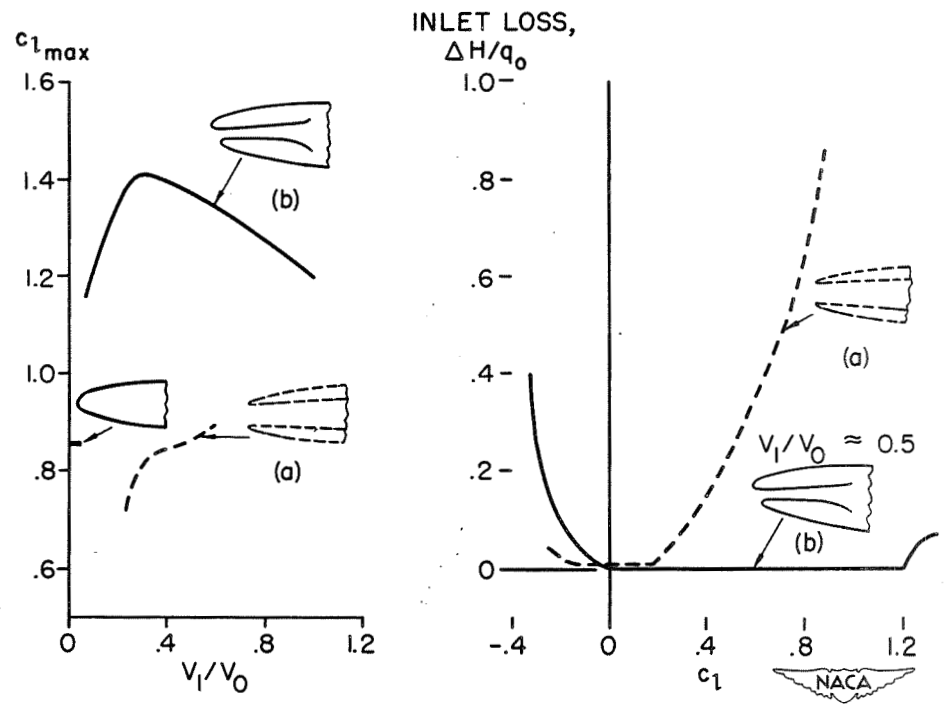
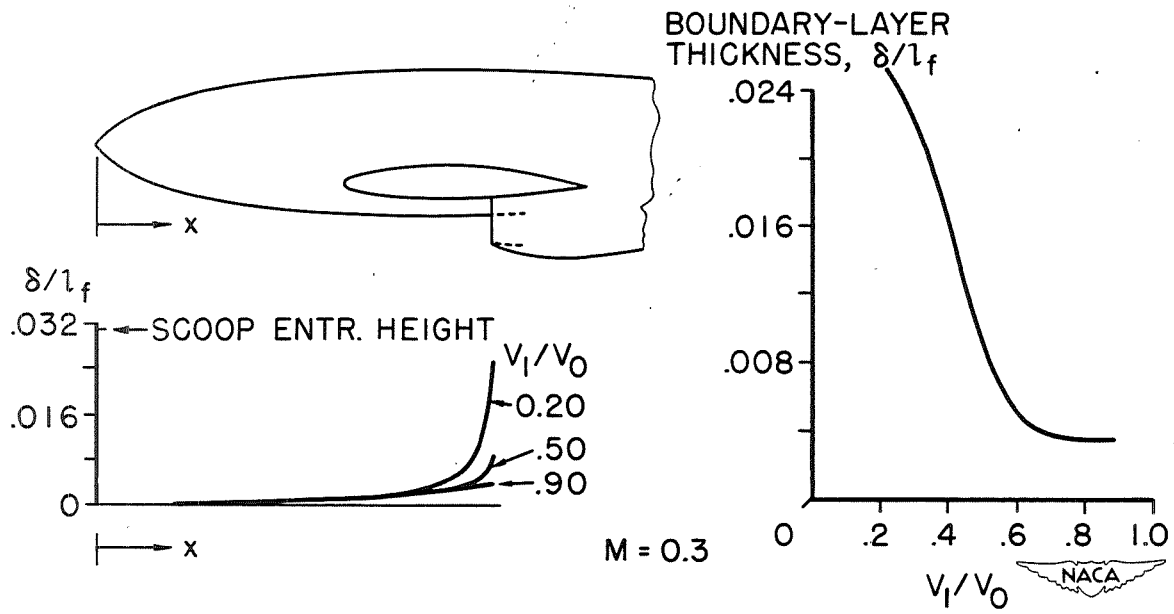Figure 8.- Maximum lift and inlet losses for two wing inlets.
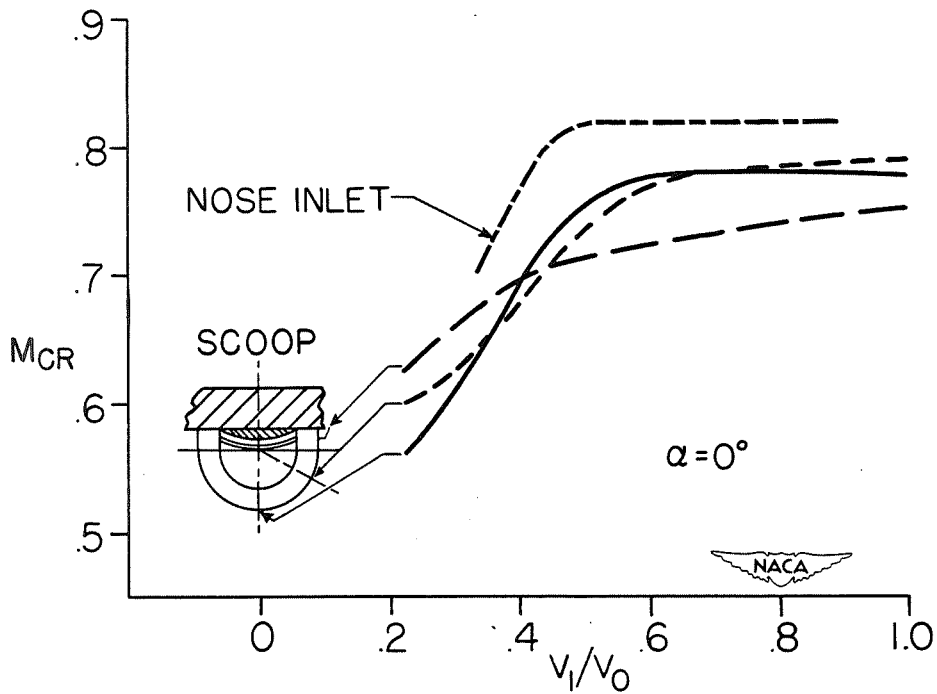
BOUNDARY-LAYER
THICKNESS, δ/l_f

.024

.016

.008

δ/l_f

.032 ← SCOOP ENTR. HEIGHT

V_I/V_0

0.20

.50

.90

.016

0

M = 0.3

0   .2   .4   .6   .8   1.0

V_I/V_0

NACA

Figure 9.- Boundary-layer thickness ahead of fuselage scoop.

.9

.8

NOSE INLET

.7

M_{CR}

SCOOP

.6

$\alpha = 0°$

.5

NACA

0   .2   .4   .6   .8   1.0

V_I/V_0

Figure 10.- Critical Mach numbers of nose inlet and scoop.
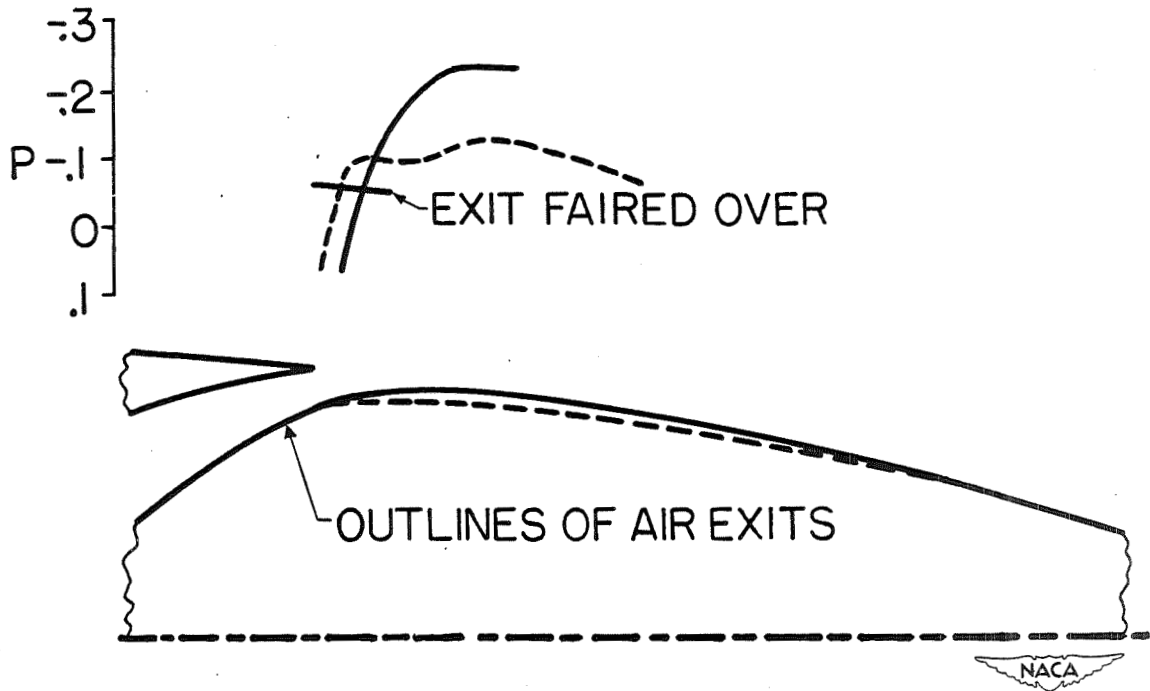
Figure 11.- Pressure distributions over air exits.
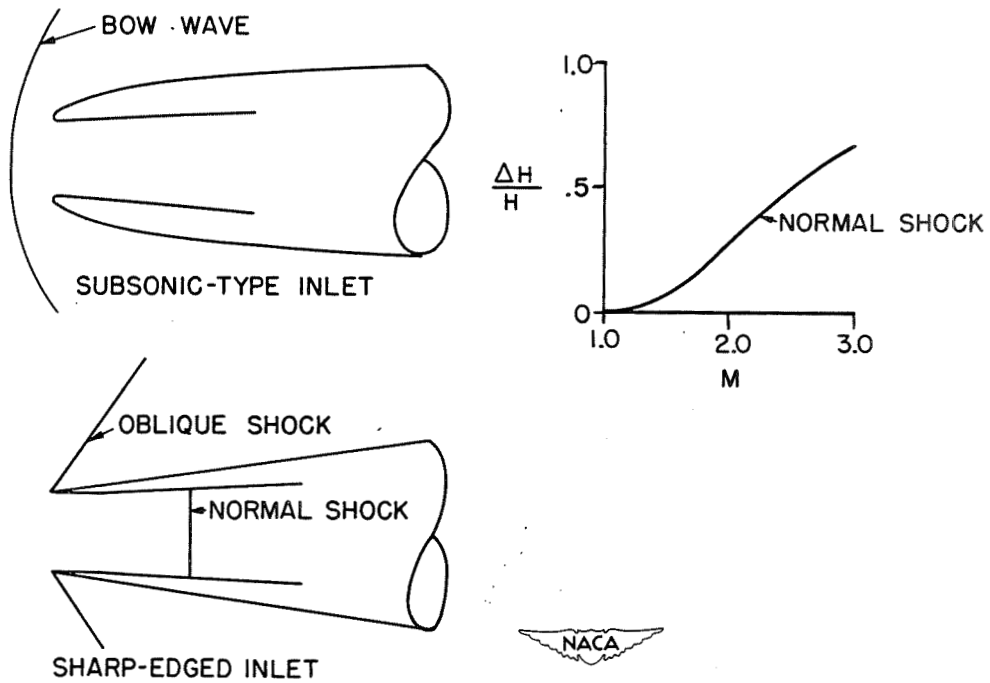
Figure 12.- Air inlets at supersonic speeds.

THROAT CONTRACTION
RATIO

NORMAL SHOCK

CONVERGING-DIVERGING
DIFFUSER

REQUIRED FOR COMPRESSION
TO M = 1

MAXIMUM PERMISSIBLE
FOR SHOCK ENTRANCE
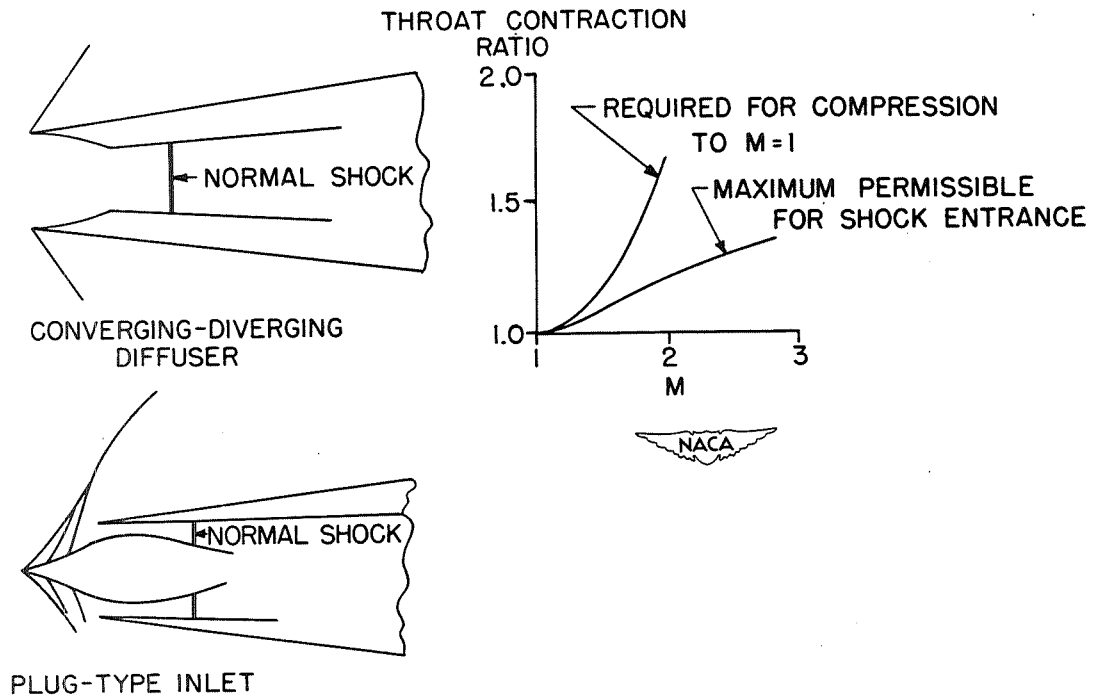
2.0

1.5

1.0

1   2   3
M

NACA

NORMAL SHOCK

PLUG-TYPE INLET

Figure 13.- Air inlets at supersonic speeds.